View metadata, citation and similar papers at core.ac.uk

brought to you by CORE

provided by Caltech Authors - Main

© 2020 Wiley-VCH GmbH

ADVANCED MATERIALS TECHNOLOGIES

Supporting Information

for *Adv. Mater. Technol.*, DOI: 10.1002/admt.202000791

Hydrogel-Based Additive Manufacturing of Lithium Cobalt Oxide

Daryl W. Yee, Michael A. Citrin, Zane W. Taylor, Max A. Saccone, Victoria L. Tovmasyan, and Julia R. Greer*

Copyright WILEY-VCH Verlag GmbH & Co. KGaA, 69469 Weinheim, Germany, 2020.

Supporting Information

Hydrogel-based Additive Manufacturing of Lithium Cobalt Oxide

Daryl W. Yee, Michael A. Citrin, Zane W. Taylor, Max A. Saccone, Victoria L. Tovmasyan, Julia R. Greer.*

Theoretical shrinkage and mass loss

The theoretical shrinkage can be determined, to a first approximation, by making the following assumptions: 1) Each mol of Li^+ and Co^{2+} in the Li^+/Co^{2+} hydrogel is combined into a mol of lithium cobalt oxide (LCO). 2) All other components in the hydrogel precursor are removed during the combustion process, and leave negligible amounts of mass behind. 3) Aside from the changes in dimension from shrinkage, the net shape of the polymer is kept.

The concentration of cobalt nitrate hexahydrate, c_{Co} in the resin can be determined by:

$$c_{Co} = \frac{m_{Co,resin}}{V_{resin}}$$

where $m_{Co,resin}$ is the mass of cobalt nitrate hexahydrate in the prepared resin of volume V_{resin}.

For simplicity, we will print a sphere of radius $R_{printed}$ with volume $V_{printed}$. The mass, $m_{Co,printed}$, and number of moles of cobalt nitrate, $mol_{Co,printed}$, in the printed volume, is then given by:

$$m_{Co,printed} = c_{Co} \times V_{printed}$$

$$mol_{Co,printed} = \frac{m_{Co,printed}}{Mw_{Co}}$$

where Mw_{Co} is the molecular weight of cobalt nitrate hexahydrate.

Assuming that each mole of cobalt nitrate hexahydrate is fully converted to a mole of LCO, the number of moles of LCO, $mol_{LCO,printed}$, after calcination will be equivalent:

$$mol_{LCO,printed} = mol_{Co,printed}$$

The volume of LCO, $V_{LCO,printed}$ can then be determined using the bulk density, ρ_{LCO}, and molecular weight of LCO, Mw_{LCO}:

$$V_{LCO,printed} = \frac{mol_{LCO,printed} \times Mw_{LCO}}{\rho_{LCO}}$$

Assuming net shape conversion, the radius of the LCO sphere can be calculated and, the ratio of R_{LCO} to $R_{printed}$ determined by:

$$\frac{R_{LCO}}{R_{printed}} = \sqrt[3]{\frac{V_{LCO,printed}}{V_{printed}}}$$

The linear shrinkage can then be represented by:

$$Shrinkage = \left(1 - \frac{R_{LCO}}{R_{printed}}\right) \times 100$$

and simplified into:

$$Shrinkage = \left(1 - \sqrt[3]{\frac{m_{Co,resin} \times Mw_{LCO}}{V_{resin} \times Mw_{Co} \times \rho_{LCO}}}\right) \times 100 \qquad \textbf{(Equation S1)}$$

For example, for n_{PEGda} ~ 2.2 (where n_{PEGda} is the mol ratio of poly(ethylene glycol) diacrylate to cobalt nitrate hexahydrate) , the lithium and cobalt nitrate-containing photoresin contained 15.55g of cobalt nitrate hexahydrate in 110ml of photoresin. The molecular weight of LCO and cobalt nitrate hexahydrate was determined to be 97.87g/mol and 291.3g/mol respectively. The density of bulk LCO was taken to be 5.05g/cm^3.[1] Using the Equation S1 derived above, the theoretical linear shrinkage was determined to be 79%.

The theoretical mass loss can also be determined by making similar assumptions, and can be approximated by:

$$Mass\ Loss = \left(1 - \frac{m_{Co,resin} \times Mw_{LCO}}{Mw_{Co} \times m_{resin}}\right) \times 100 \qquad \textbf{(Equation S2)}$$

where $m_{Co,resin}$ is the mass of the cobalt nitrate hexahydrate salt in the resin, Mw_{LCO} is the molecular weight of LCO, Mw_{Co} is the molecular weight of cobalt nitrate hexahydrate, and m_{resin} is the mass of resin after preparation. Table S1 below indicates the theoretical linear shrinkage and mass loss values for the resins with different n_{PEGda} values. n_{PEGda} denotes the mol ratio of the polymer binder, PEGda to the cobalt nitrate hexahydrate salt.

Table S1. Theoretical linear shrinkage and mass loss values for the resins with different n_{PEGda} values

Approximate n_{PEGda}	Theoretical shrinkage (%)	Theoretical Mass loss (%)
2.2	78.9	95.8
1.0	75.8	93.9
0.5	74.0	92.5
0.4	73.4	92.0

Discussion on porosity for n_{PEGda} ~ 0.4 lattices

The n_{PEGda} ~ 0.4 (LCO-s and LCO-e) lattices were observed to have the densest microstructures, having no large pores and the smallest cracks. However, the presence of micropores was still observed in the cross-sections and surface microstructures (Figure 2b-d). The experimental shrinkage and mass loss of the LCO structures were found to be 43.8% and 92.2% respectively. From Table S1, the experimentally determined mass loss was similar to the theoretically evaluated value, but the shrinkage value was significantly different. Taken

together, we can conclude that the discrepancy between the theoretical and experimental shrinkage can be attributed to the porosity in the material.

One approach to estimating the porosity is to compare the measured mass of the lattice to the expected mass of the lattice based on the volume of the structure. The calcined lattices had on average, beam thicknesses of 100µm and a unit cell length of 500µm. Using a computer-aided design model to construct a lattice with the same number of unit cells but with these dimensions, we obtain a theoretical mass of 68.4mg (based on the volume of the lattice, 13.54mm^3, and the density of LCO at 5.05mg/mm^3). On average, the measured mass of the lattices was 29.9mg. From the ratio of the measured mass and the mass expected based on the volume of the structure, we can determine that the structures had an estimated microscale porosity of 56.3%.

The porosity can also be estimated by comparing the actual linear shrinkage to the theoretical shrinkage. By using the ratio of the diameter of the expected size of the lattice (26.5% of the original diameter) to the actual size of the lattice (56.3% of the original diameter), we can estimate the porosity to be 52.9%, which is consistent with the value from the mass approach. The porosity can potentially be decreased by: a) using even lower values of n_{PEGda}, b) higher concentrations of metal salts, and c) the use of a post-calcination sintering step to densify the material.

The microscale porosity of the cross-section of the lattice (Figure 2d), as determined by ImageJ analysis, was approximately 31%. The discrepancy between this number and the calculated porosity of ~55% can be attributed to the following: presence of cracks in the structures as can be seen in Fig. 2c, d. The presence of pores on the surface of the beams (Figure 2b) and non-uniform shrinkage of the beams will also account for some of this discrepancy. The accuracy of the ImageJ analysis is also influenced by the choice of the threshold brightness value that is used to distinguish between a grain and a pore. Given that the cross-sections are imaged at an angle, with shadowing effects due to the surrounding materials, the brightness of the cross-section is not constant throughout the height of the cross-section image. Consequently, the brightness threshold value is not constant throughout the field of view.

Surface microstructure of n_{PEGda} ~2,2 and 1.0 LCO lattices

Figure S1 shows a representative scanning electron microscope (SEM) image of the surface of LCO lattices made with either the n_{PEGda} ~2.2 or 1.0 resins.

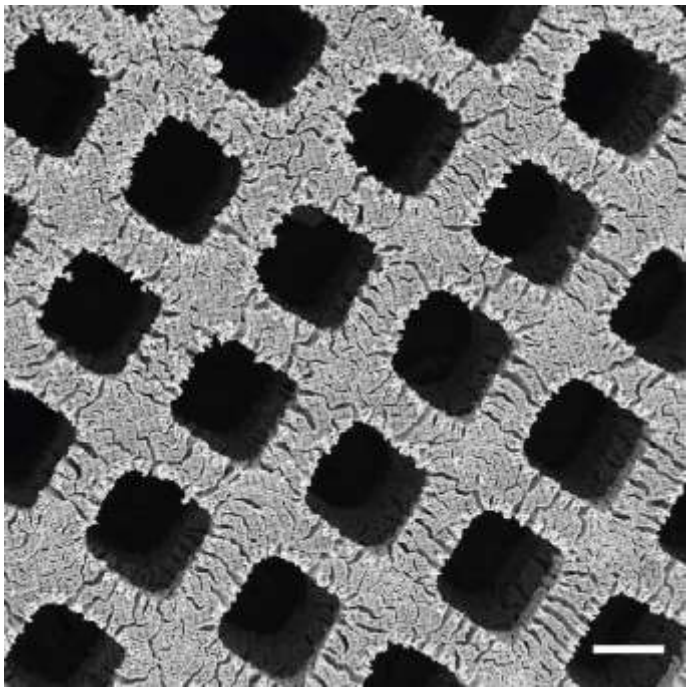

Figure S1. Representative SEM image of the surface of LCO lattices made with n_{PEGda} ~ 2.2 or 1.0 resins. Scale bar, 200μm

Optical image of as-printed Li^{+}/Co^{2+} hydrogel structures

Figure S2 shows a representative optical image of the surface of the as-printed hydrogel structures. The diamond array pattern can clearly be seen, indicating that the array seen on the calcined structures are artefacts from the print process. The diamond array likely reflects the pixel array of the DLP printer.

Figure S2. Representative optical image of the surface of the as-printed hydrogel structure, regardless of n_{PEGda} value. The diamond array can be clearly seen throughout the structure. Scale bar, 200µm.

Unit cell parameters as calculated from X-ray diffraction (XRD)

Table S2. Unit cell parameters of LCO-s and LCO-e lattices

Sample	c (Å)	a (Å)	c/a
LCO-s	14.018	2.814	4.982
LCO-e	14.018	2.814	4.982

Energy-dispersive X-ray spectroscopy (EDS) spectrum

The EDS spectrum taken from the surface of the LCO-e lattices is shown below in Figure S3. Li could not be detected in our EDS setup. The combined at% of impurities was 7.5at%, assuming an equivalent percentage of Li and Co. The impurities can be attributed to the following: carbon — incompletely combusted organic material or surface carbon. Phosphorus — LAP photoinitiator. Sulfur — tartrazine UV blocker. Sodium — counter-ion of tartrazine. Aluminum and silicon — residue from the quartz tube/contaminant from mounting the sample. Quantitative elemental data from EDS is relatively inaccurate for light elements, such as oxygen and the impurities detected, so the exact percentage of impurities might vary by a few at%.

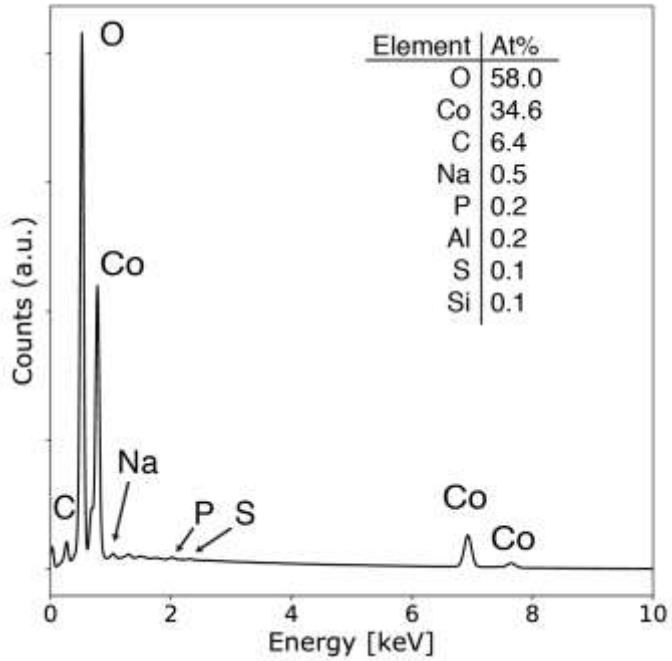

Figure S3. EDS spectrum of the surface of the LCO-e lattices. The at% of each element detected is also displayed.

Nyquist plots for LCO-e lattices

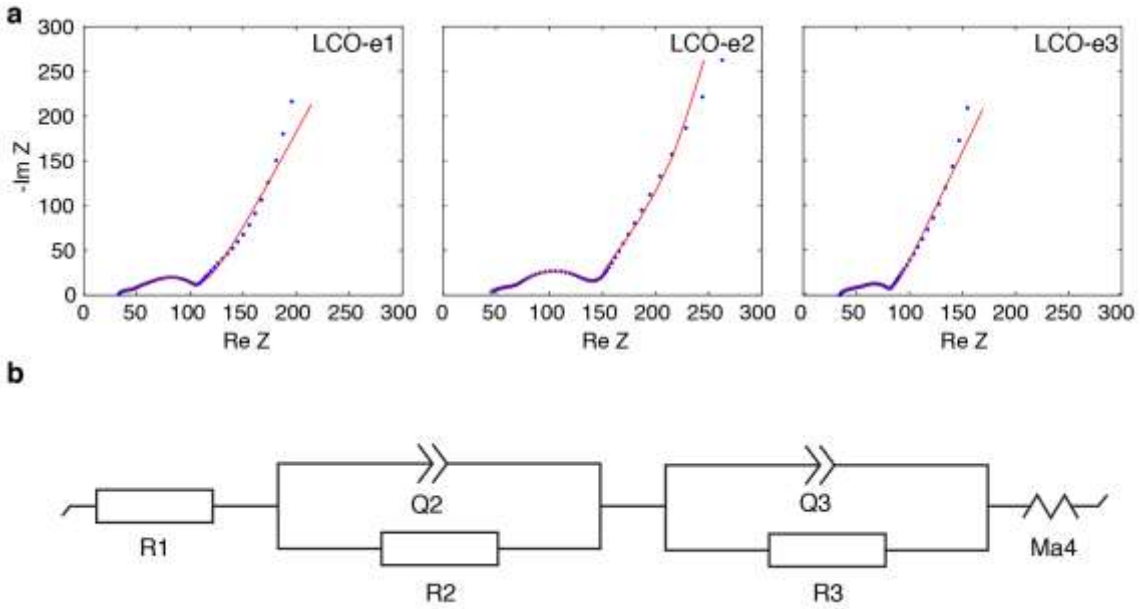

Figure S4. Nyquist plots for LCO-e(1-3) cells after electrochemical cycling, as described in Figure 4b in the main text. **(a)** Electrochemical impedance spectroscopy (EIS) was performed with a sinusoidal amplitude of 10 mV over a frequency range from 500 kHz to 100 mHz. **(b)** The equivalent circuit contains R1 (ohmic resistance), two parallel constant phase element (CPE)/resistor elements, and an anomalous diffusion element. The EIS data were fit using the equivalent circuit with the Z Fit function of EC-Lab. The results for the fits for the resistor elements are provided in Table S3.

Table S3. Results for the fits for the resistor elements using the Z Fit function of EC-Lab.

Sample	R1	R2	R3
LCO-e1	26.85	26.49	55.96
LCO-e2	41.27	34.67	72.96
LCO-e3	35.37	4.20	45.3

Coin cell setup

Figure S5. Schematic of the coin cell stack in the 2032 size coin cells.

Compositions of the resins with different n_{PEGda} values

The compositions of the resins with the different n_{PEGda} values are shown below in Table S4. The different n_{PEGda} values were achieved by changing the volume ratios of metal salt precursors and PEGda used in the resin. The LAP and TZ were dissolved in the water before being added to the metal salt-PEGda solution.

Table S4. Composition of resins prepared

nPEGda	2.67M Li soln (mL)	2.67M Co soln (mL)	PEGda (mL)	LAP (mg)	TZ (mg)	Water (mL)
2.2	20.0	20.0	60.0	250	50	10.0
1.0	30.0	30.0	40.0	250	50	10.0
0.5	37.5	37.5	25.0	250	50	10.0
0.4	40.0	40.0	20.0	250	50	10.0
0.4 (Li excess)	42.0	40.0	20.0	255	51	10.2

Print parameters for cubic lattice

The CAD model of the file is shown below in Figure S6, along with the two pattern slices that make up the entire structure. The exposure parameters used for DLP printing with the Autodesk Ember is shown in Table S5 below. No "Burn-in" layer was used. An offset of 300μm was used after leveling.

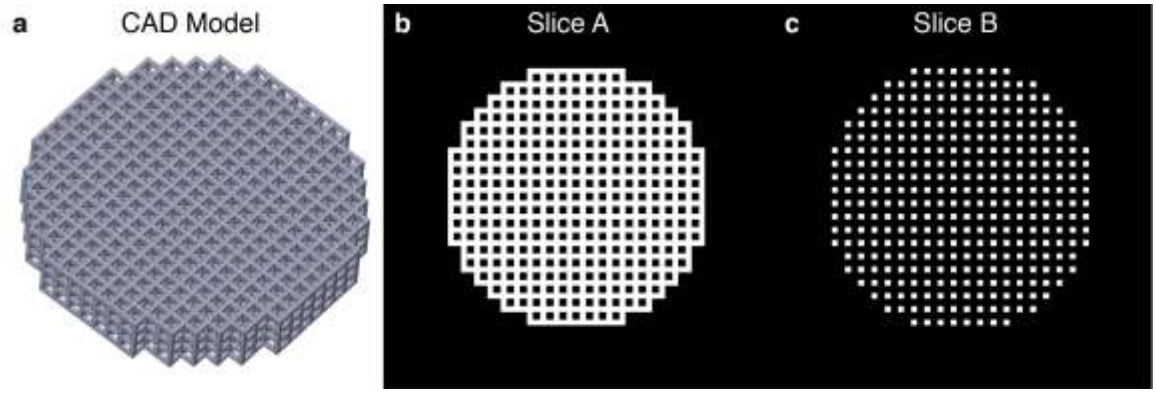

Figure S6. (a) CAD file of the cubic lattice made. **(b)** Slice A pattern. **(c)** Slice B pattern.

Table S5. Print exposure parameters used for DLP printing of the cubic lattice

Wait before exposure (s)	**Print exposure (s)**	**Slide rotation speed (RPM)**
First Layer, Slice A		
5.0	15.0	0.5
Model Layer, Slice A		
3.0	14.0	1.0
Model Layer, Slice B		
3.0	29.0	1.0

References

[1] J. Akimoto, Y. Gotoh, Y. Oosawa, *J. Solid State Chem.* **1998**, 141, 298.